

# Multipath Mitigation for Narrowband Receivers

R. Eric Phelts, Per Enge  
Department of Aeronautics and Astronautics, *Stanford University*

## ABSTRACT

Narrowband receivers are more robust to narrowband interference and to GPS signal faults, but they tend to have relatively poor multipath performance. Few current techniques are capable of mitigating multipath in these receivers. The Tracking Error Compensator (TrEC) however operates independent of the receiver's precorrelation bandwidth (PCB) using the concept of Multipath Invariance (MPI).

Theoretical bandlimited mitigation performance curves for this approach were generated and compared to those of a conventional delay-lock loop. The effects of a narrow PCB on the TrEC were experimentally investigated. A practical TrEC algorithm was developed and implemented on a Mitel Semiconductor receiver having a 2MHz PCB. The performance curves and accompanying statistics were validated for short-delay multipath using a GPS signal generator to generate multipath with known characteristics on a prescribed pseudorange. Measured pseudorange errors were compared to those estimated by the TrEC in real-time. For the same case, position errors resulting from short and long time-constant carrier smoothing and were contrasted with those from the TrEC algorithm. This data suggests that it may be possible to significantly improve the multipath mitigation performance of narrowband receivers.

## INTRODUCTION

For GPS users, multipath (MP) is caused by reflections of the satellite signal from the ground or from nearby buildings or other obstacles. Multipath errors result when the receiver receives the direct or line-of-sight (LOS) satellite signal via multiple paths and processes the combined signal as if it were only the direct. These errors are particularly difficult to remove since, in general, the following is true:

- 1) The pseudorange measurement is derived from a code-tracking delay-lock loop (DLL).
- 2) Pseudorange errors due to multipath, in general are nonlinear functions of MP amplitude delay, phase and phase rate [1].
- 3) Multipath errors are not zero-mean [2].

- 4) Multipath is not spatially correlated.

For 2MHz narrow-precorrelation bandwidth (PCB) receivers, a 0.5-chip correlator pair is commonly used for tracking yet there is relatively little advantage to using a narrow correlator in a receiver with such a narrow front-end bandwidth (See Figure 1.). Accordingly, any wide-PCB, narrow correlator-based WAAS receivers tracking the 2.2MHz-bandlimited geostationary (GEO) satellite will have this relatively poor multipath performance. In addition, since for many users the GEO is at low elevation angles and is essentially stationary for static users, the multipath problem could be even more significant.

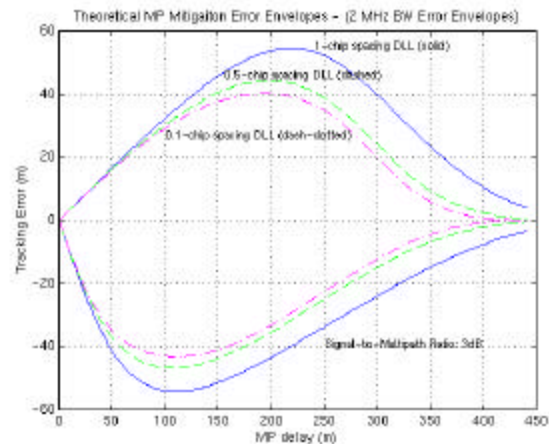
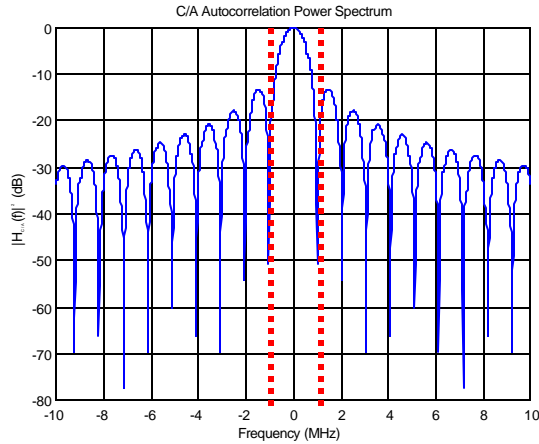


Figure 1. DLL Tracking error vs. MP relative delay for 2MHz bandwidth receivers

This paper addresses the problem of mitigating multipath in these narrow-PCB receivers. The term narrowband will apply to receivers having a (two-sided) PCB less than 2.5MHz wide. These narrowband receivers pass only the main lobe of the C/A code power spectrum (See Figure 2). All others will be considered wideband.



**Figure 2. C/A Autocorrelation Power Spectrum Envelope.**

## BACKGROUND

### *Narrowband Interference*

In general, narrowband interference has a bandwidth  $\ll 1\text{MHz}$  [1]. This type of interference consists of both intentional and unintentional continuous wave (CW) sources including transmitter harmonics from CB's and AM and FM stations.

Although a CW interferer is unlikely to cause long-term navigation problems under most circumstances [1], [3], [4], interference with wider bandwidths (e.g.  $>10\text{kHz}$ ) could be significantly more dangerous. For high-integrity systems like the Local Area Augmentation System (LAAS), this susceptibility to interference could be a critical liability [5].

### *Evil Waveforms*

Satellite-signal anomalies or “evil waveforms” (EWF's) result from a failure of the signal generating hardware on one of the GPS space vehicles (SV's). Typically, these anomalies may cause severe distortions of the autocorrelation peak inside GPS receivers. In local area differential systems, undetected evil waveforms may result in large pseudorange errors, which in general do not cancel. One such failure occurred on SV19 in October of 1993. It caused differential pseudorange errors on the order of 3 to 8 meters. Undetected errors of this size are much too large for aircraft conducting a precision approach [7].

For designing a signal quality monitoring (SQM) and detection scheme, an evil waveform model was developed. This model assumes the anomalous waveform is some combination of second-order ringing (an analog failure mode) and a lead/lag (digital failure mode) of the

pseudorandom noise (PRN) code chips [7]. A good ground monitoring implementation would detect any and all waveforms that would result in large differential PRE's.

If an EWF is undetected by a particular SQM scheme, it is necessary to determine the impact on the differential PRE's of airborne users. These users may have varied receiver implementations, and in general, receiver manufacturers desire the freedom to implement both narrow and wide PCB's with narrow and/or wide correlator spacings. For LAAS, the current goal for Category I precision approaches is to protect an L-shaped region of this two-dimensional user design space using a practical ground monitoring scheme [6]. To meet the requirements, the maximum PRE's within these regions must be less than 3.5 meters.

## MOTIVATION

### *Narrowband Interference*

A complete explanation of assumptions and equations for determining a receiver's nominal resistance to jamming and are given in [4]. For suppressing wideband interference, narrowband receivers have a negligible advantage [6]. Conversely, for narrowband interference, the differences in vulnerability can be significant. Figure 3 summarizes the advantages of a 2MHz-PCB receiver over three wider-PCB ones in terms of the amount of attenuation they apply to such interferers at frequency offsets greater than 1MHz. In fact, if the EMI is offset 2MHz or more from L1, a 2MHz receiver can provide many orders of magnitude more attenuation than the 8, 16 and 20MHz ones. The larger the frequency offset of the interference, the greater the advantage of narrowband receivers

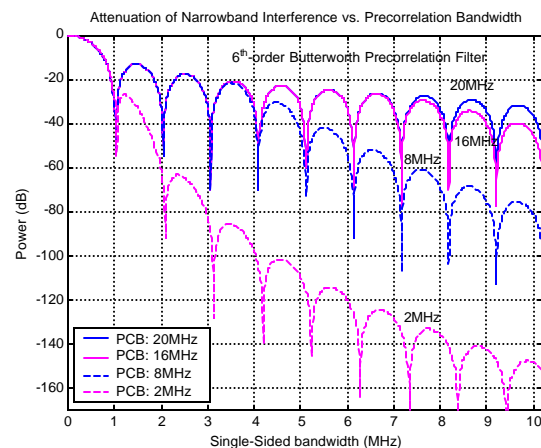


**Figure 3. Relative attenuation of narrowband interference for 4 different PCB's.**

## Evil Waveforms

Using the equations and assumptions given in [7], [the three standard digital and analog threat models were used to evaluate robustness of airborne user receivers to evil waveforms in [6]. Assuming all evil waveforms within each threat model were undetected (no SQM was used, the results can be summarized as follows:

- Only the “nearly-matched” consistently have receivers have small PRE’s.
- Narrowband receivers generally have maximum PRE’s less than or equal to those of most wideband receivers.
- Narrowband receivers perform best against high-frequency ringing failures (See Figure 4).

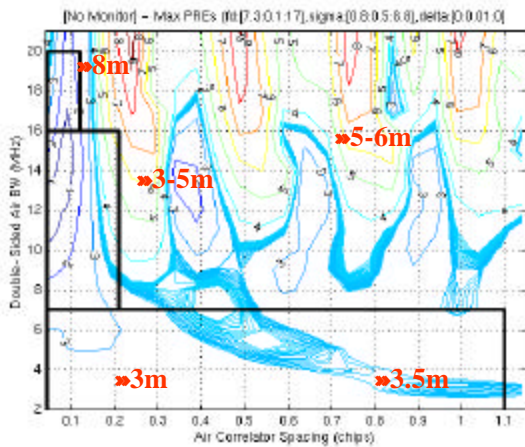


Figure 4. TM B: Maximum PRE’s for airborne users. ( $f_{d,min}=7.3\text{MHz}$ )

## TRACKING ERROR COMPENSATOR (TrEC)

### Multipath Invariance

The Tracking Error Compensator (TrEC) is a multipath mitigation approach that leverages the concept of Multipath Invariance (MPI) to operate independent of the receiver PCB. The premise of MPI is that there exist regions and/or properties of the autocorrelation function that do not vary as a function of the multipath parameters. These multipath *invariant* regions and/or points are located at the plateaus of the autocorrelation function of a particular PRN code sequence (See Figure 5). Note that these MPI plateaus are not always located adjacent to the peak.

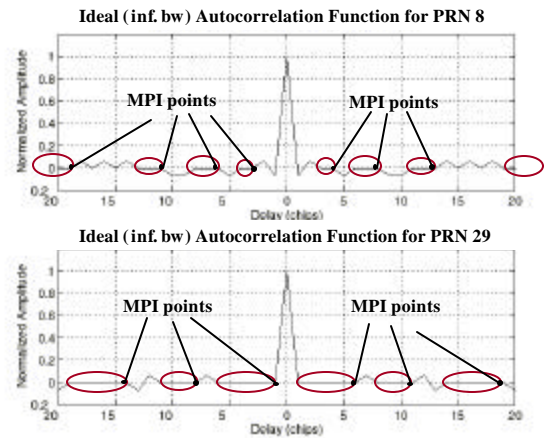


Figure 5. Normalized ideal autocorrelations showing MP Invariant Plateaus and Points.

More details on the MPI concept and its assumptions can be found in [8], however the general algorithm for the TrEC is as follows:

- 1) Generate (offline) the ideal autocorrelation functions corresponding to each PRN and compose a look-table corresponding to the ideal distance between the peak

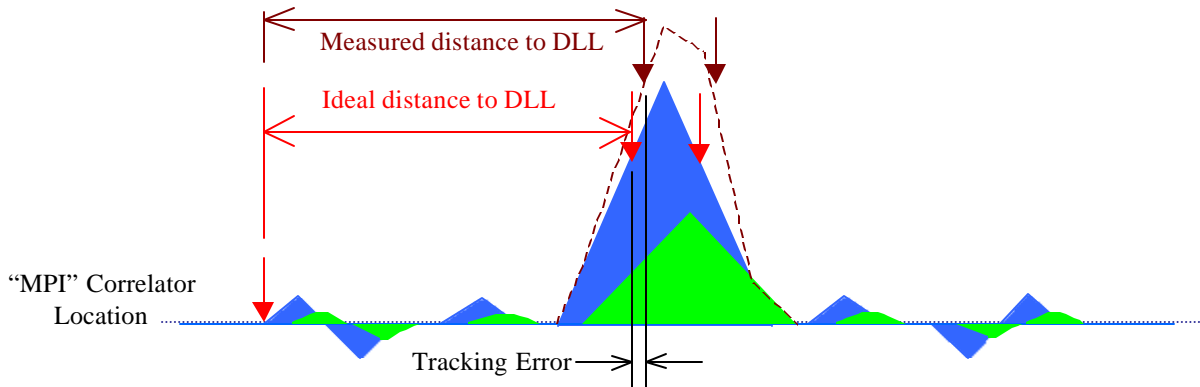


Figure 6. The Tracking Error Compensator (TrEC): Updating the primary DLL tracking solution with the corrected, relative position to the MPI point.

and the MPI point.

- 2) Once the receiver is tracking a satellite in a given channel, use knowledge of the ideal distance to the MPI location for the corresponding PRN and reasonable bounds on the current tracking error to bound the desired point.
- 3) Search and optimize within the localized region of the autocorrelation function to find the location of the MPI point with respect to the primary (tracking) correlators.
- 4) Once the point is identified, correct the tracking loop solution by the difference between the Measured and Ideal DLL positions. (See Figure 6.)

### Tracking Error Performance

The performance curves differ for the TrEC in that they are not really “envelopes”. The theoretical TrEC envelope is actually straight line, offset by bias that can be calibrated out. If a bias remains, provided the same compensation is performed on every valid pseudorange, it will simply become a part of the clock bias in the navigation solution and will not affect the final position solution. The theoretical performance curves for the noise-free, 2MHz-bandlimited case is shown below in Figure 7.

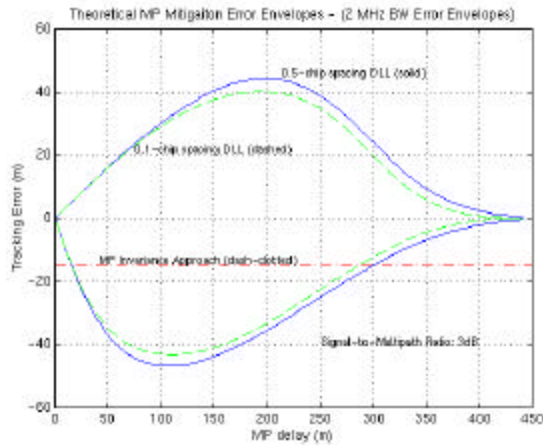
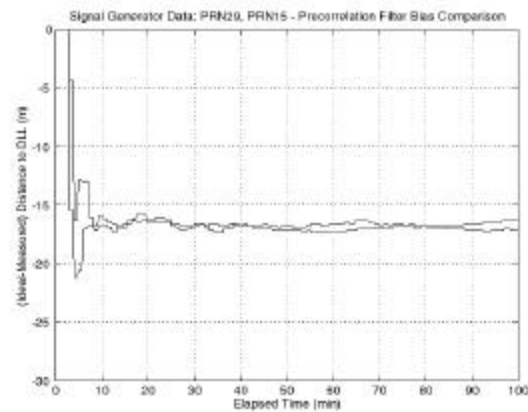


**Figure 7. MPI Approach and DLL Tracking error vs. MP relative delay for 2MHz bandwidth**

An actual bias estimate (for one particular TrEC implementation) was made using a Welnavigate GPS Signal Generator and is shown in Figure 8. As stated previously, the bias is independent of relative MPI point location and PRN number. Note, however that the convergence time for this TrEC was approximately 5 minutes. This convergence time translates directly to the initialization time required by the TrEC algorithm prior to making valid, real-time corrections to the DLL. This time can be shortened (or lengthened) depending on the actual implementation assumptions and/or requirements of the

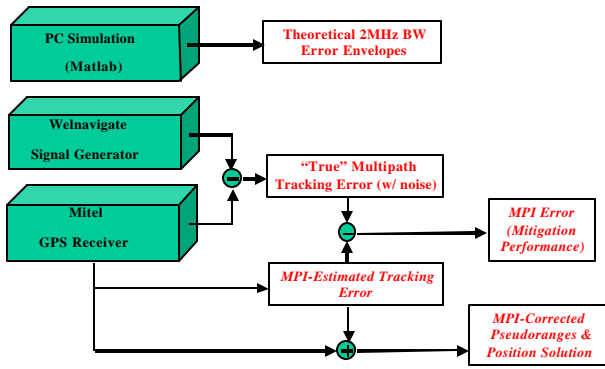
TrEC. However, these details are beyond the scope of this paper.

Assuming the multipath has relatively short relative delay—the most troublesome multipath—we verified these performance curves using the Welnavigate GPS Signal Generator. It was capable of simulating not only the entire GPS satellite constellation, but also of generating multipath (with known parameters) on a given pseudorange. This latter feature was used to experimentally verify the short-delay multipath performance of a narrowband received implementing the MPI approach. The algorithm was implemented on a Mitel Semiconductor (formerly GEC Plessey) receiver with a front-end bandwidth of 2MHz and a 0.5-chip correlator spacing.



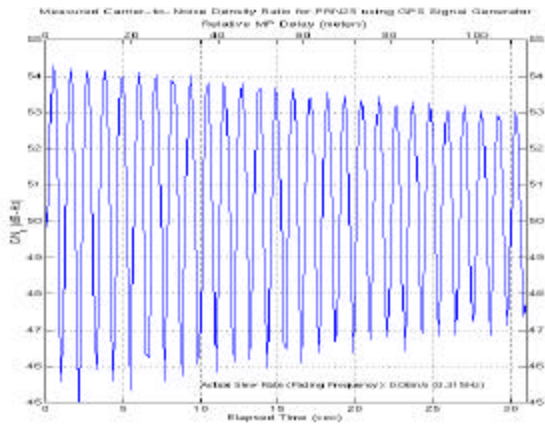
**Figure 8. PCB filter bias comparison for PRN25 and PRN29 (Signal Generator Data).**

Figure 9 illustrates the experimental setup. The signal generator was used to output the GPS satellite signals. A high post-correlation carrier-to-noise density ratio (50 to 53 dB-Hz as measured by a Novatel receiver) was used for all SV’s. A single pseudorange (PRN25) was selected to be the corrupted by multipath appropriate for generating the performance curves. The measured pseudoranges were obtained from the Mitel receiver. The “true” pseudoranges (retrieved from the signal generator truth file) were then subtracted from the measured ranges. A single inter-channel difference was performed to remove the clock bias. Only variations due thermal noise and the bias due to multipath remained.



**Figure 9. Setup for MP performance validation experiment.**

The multipath was programmed to slew at a rate of 3.6 meters/min starting from a relative delay of 0 meters. The signal-to multipath ratio (SMR) was 3dB. The effect of these specifications on the received signal power is illustrated in Figure 10. Note that the high signal power of the MP signal induced correlation peak amplitude swings of approximately 9dB at a relative MP delay of 0 meters. Also note that the data shown was subsampled for clarity. The actual “fading” frequency of the combined multipath-plus-direct signal is higher than that depicted.



**Figure 10.  $C/N_0$  for PRN25 during programmed multipath slew (Fading frequency shown aliased).**

The top plot in Figure 11 shows the true multipath tracking error compared to the MPI-measured tracking error. Using the Mitel receiver, the MPI algorithm measured the tracking error in real-time. Note that at approximately  $t=10$  minutes, the tracking loop temporarily lost lock on SV 25. A momentary fault in the generated signal caused this outage. It occurred at the same time for each trial and forced the MPI routine to reinitialize. (Note that the outages partially affected the resulting performance curve, since about 5 minutes were required for the routine to re-converge to the

proper MPI point and resume making valid pseudorange corrections.) The second plot shows both the raw and carrier-smoothed (128-sec) differences between the actual and measured tracking errors. The carrier-smoothed curve is the performance curve for the MPI approach for this particular trial (See bottom plot of Fig. 11). The mean of this curve is 1.18 meters and its standard deviation is 2.45 meters.

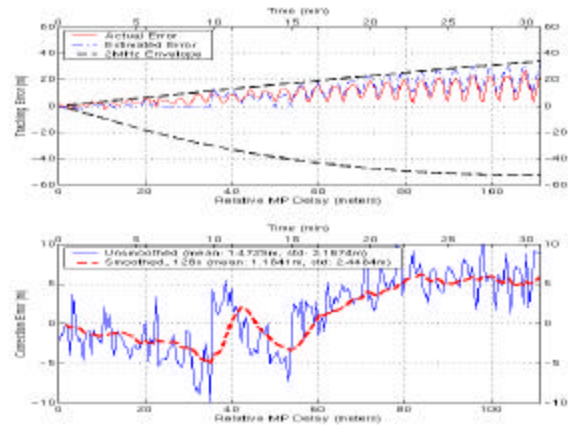


**Figure 11. Measured error and true error**

In order to validate the theoretical performance curve (the straight line) of Figure 7, data was taken from 10 trials. The results are plotted in Figure 12 and the corresponding statistics are summarized in Figure 13. The mean bias (for this TrEC implementation) is approximately -2.5m. Accounting for the increased variance due to the single-difference, the average smoothed and unsmoothed standard deviations are 1.4m and 3.2m respectively. Significant perturbations occurred, however, because of the temporary signal outage on SV25, so the true (undisturbed) standard deviation of the performance curves is actually smaller than that reported here.

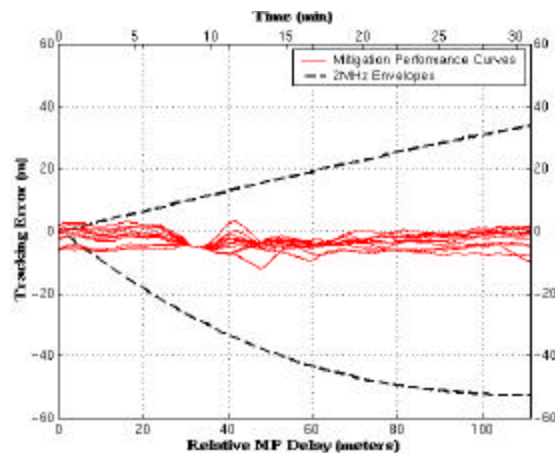


**Figure 12. Short-delay TrEC performance curves (10 trials, 1-Hz data)**

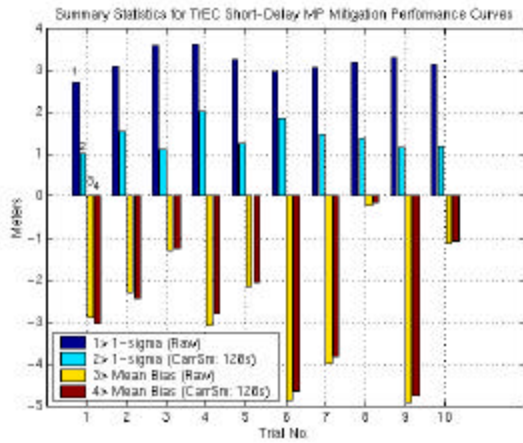


**Figure 13. Short-delay TrEC performance statistics (10 trials, 1Hz data)**

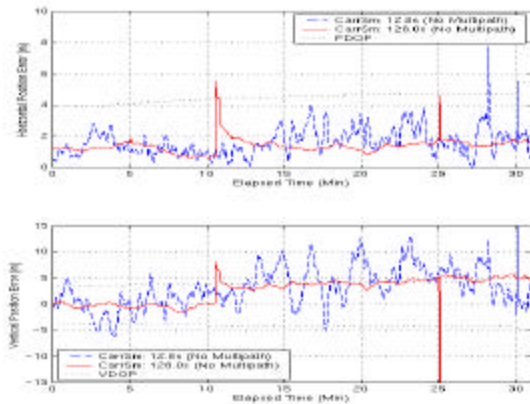


**Figure 14. Nominal Mitel position errors (no multipath).**

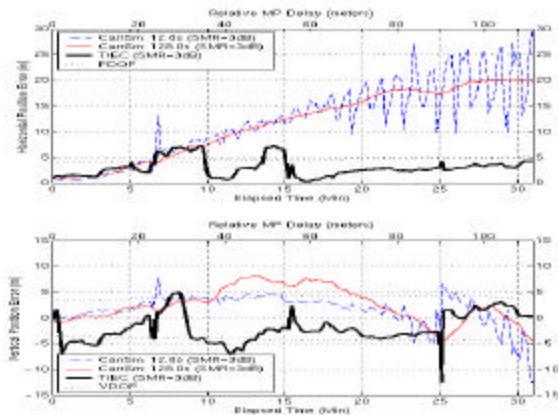


**Figure 15. Mitel position errors with and without TrEC (multipath added, SMR=3dB).**

### Position Error Performance

In addition to thermal noise errors, the pseudoranges generated by the Welnavigate contained only a small, slowly-varying ionospheric error that ranged from 3-5 meters. No Selective Availability (SA) or troposphere errors were added. By applying the TrEC corrections to the multipath-corrupted pseudoranges to be used in the navigation solution, the position-domain performance of the TrEC was examined.

The top and bottom plots of Figure 14 show the (nominal, zero-multipath) horizontal and vertical position errors, respectively for the Mitel receiver for a single trial. Each plot shows both the nominal errors for a small smoothing time constant (12.8s—nominal for the Mitel) and a large one (128.0s) as a function of time. Also depicted are the PDOP and VDOP values. Note that there are other small signal “glitches” that occurred during the trial (at  $t \approx 11$ min and  $t \approx 25$ min). Although they resulted brief jumps in horizontal and vertical position errors, the faults did not occur on PRN25, hence the TrEC performance was not impacted.

Figure 15 shows the same Mitel position errors for the case where multipath has been added as described in the previous section. Here, however, the carrier smoothed-only errors are contrasted against those of the TrEC-corrected position solution. (The nominal smoothing time of 12.8 seconds was used for the TrEC-corrected pseudoranges.) For the horizontal position errors, the TrEC was capable of removing the large bias, where the carrier smoothing alone was not. In fact it suffered its worse position errors between  $t \approx 5$ min and  $t \approx 15$  min. The first large excursion occurred due to the reinitialization previously discussed. This lasted for approximately 4-5 minutes as the TrEC was reinitialized. The second excursion occurred shortly thereafter—while the TrEC was converging/refining on its estimate of the MPI location. Neglecting the discontinuity at  $t \approx 25$ min, the vertical position errors remain relatively small and consistent for all the implementations this entire range of MP delays.

## CONCLUSIONS

Few current multipath mitigation techniques are applicable to narrowband receivers. The Tracking Error Compensation technique was experimentally validated as narrow PCB-capable multipath mitigation technique. Measured performance curves validate the theoretical

constant error envelopes for short-delay multipath. These results indicate the TrEC may provide significant tracking error performance gains over the standard correlator techniques for these receivers.

Preliminary position domain results support the assertion that the TrEC is capable of removing the MP biases. In this data shows that addition any remaining TrEC-implementation offset due to finite PCB does not affect the position solution.

## REFERENCES

- [1] Parkinson, B. W., Spilker, J. J., Eds., *Global Positioning System: Theory and Applications*, Vol. 1, pp. 547-68, 717-55, Washington, DC, USA, American Institute of Aeronautics and Astronautics, 1996.
- [2] Van Nee, D. J. R., 1992, "Multipath Effects on GPS Code Phase Measurements," *NAVIGATION, Journal of Navigation*, Vol. 39, No. 2, pp. 177-90.
- [3] Ndili, A., *Robust Autonomous Signal Quality Monitoring*, Ph.D. thesis, Stanford University, Stanford, California 94305, August 1998.
- [4] Kaplan, E. D., *Understanding GPS Principles and Applications*, pp. 209-36, Artech, Boston, Massachusetts, 1996.
- [5] Corrigan, T. M., Hartranft, J. F., Levy, L. J., et al., *GPS Risk Assessment Study*. The John's Hopkins University, Applied Physics Laboratory, VS-99-007, January 1999.
- [6] Phelts, R. E., Enge, P. K., "The Case For Narrowband Receivers," *ION National Technical Meeting*, San Diego, CA, January 2000.
- [7] Enge, P. K., Phelts, R. E., Mitelman, A. M., "Detecting Anomalous signals from GPS Satellites," Report to FAA?, 1999.
- [8] Phelts, R. E., Stone, J. M., Enge, P. K., Powell, J. D., "Software-based Multipath Mitigation: Sampling for Multipath Invariance," *Program and Proceedings of the 4<sup>th</sup> International Symposium on Satellite Navigation Technology and Applications*, Session 3, 1999.
- [9] Dierendonck, A. J., Fenton, P., Ford, T., "Theory and Performance of Narrow Correlator pacing in a GPS Receiver," *NAVIGATION, Journal of the Institute of Navigation*, Vol. 39, No. 3, pp. 265-83, 1992.
- [10] Townsend, B., et al, *Performance Evaluation of the Multipath Estimating Delay Lock Loop*, *NAVIGATION, Journal of Navigation*, Vol. 42, No. 3, pp. 503-14, 1995.
- [11] Braasch, M. S., "GPS Multipath Model Validation," *Proceedings of Position Location and Navigation Symposium*, IEEE PLANS 96, pp. 672-8, 1996.